Hindawi
Journal of Nanomaterials
Volume 2017, Article ID 9298637, 8 pages
https://doi.org/10.1155/2017/9298637

Research Article

Incorporation of Boron Atoms on Graphene Grown by Chemical Vapor Deposition Using Triisopropyl Borate as a Single Precursor

E. C. Romani,[1] D. G. Larrude,[2] M. E. H. Maia da Costa,[1] G. Mariotto,[3] and F. L. Freire Jr.[1]

[1]*Department of Physics, Pontifical Catholic University of Rio de Janeiro, 22451-900 Rio de Janeiro, RJ, Brazil*
[2]*MackGraphe, Mackenzie Presbyterian University, 01302-907 São Paulo, SP, Brazil*
[3]*Department of Computer Science, University of Verona, 37134 Verona, Italy*

Correspondence should be addressed to F. L. Freire Jr.; lazaro.puc@gmail.com

Received 16 March 2017; Accepted 18 May 2017; Published 13 June 2017

Academic Editor: Zafar Iqbal

We synthesized single-layer graphene from a liquid precursor (triisopropyl borate) using a chemical vapor deposition. Optical microscopy, scanning electron microscopy, Raman spectroscopy, and X-ray photoelectron spectroscopy measurements were used for the characterization of the samples. We investigated the effects of the processing temperature and time, as well as the vapor pressure of the precursor. The B_{1s} core-level XPS spectra revealed the presence of boron atoms incorporated into substitutional sites. This result, corroborated by the observed upshift of both G and 2D bands in the Raman spectra, suggests the p-doping of single-layer graphene for the samples prepared at 1000°C and pressures in the range of 75 to 25 mTorr of the precursor vapor. Our results show that, in optimum conditions for single-layer graphene growth, that is, 1000°C and 75 mTorr for 5 minutes, we obtained samples presenting the coexistence of pristine graphene with regions of boron-doped graphene.

1. Introduction

In recent years, graphene has attracted widespread attention in scientific and technological communities due to its atomic thickness and excellent electronic, transport, and mechanical properties, which point to its many potential applications [1]. With regard to applications, graphene appears to be a very promising candidate for use in electronic nanodevices. However, the fact that pristine graphene has no band gap is the most important limitation for the development of graphene-based nanoelectronics. Substitutional doping provides an effective approach to tailor the graphene electronic band structure because it opens an energy gap between the valence and conduction band. Nitrogen and boron are the most suitable candidates to be used as dopant elements for graphene [2, 3] because of their size, which is similar to that of carbon, and the fact that there are five and three valence electrons available to form bonds with the carbon atoms, enabling n-type doping and p-type doping, respectively.

The incorporation of these dopant elements is usually accompanied by the generation of defects [4]. If, on one hand, the presence of defects can degrade transport properties in graphene, reducing the mobility of electrons or holes, on the other hand, the defects can increase the sensitivity of sensor devices based on pristine graphene [5–7]. In fact, the sensor sensitivity may be limited by the chemical inertness of graphene. Indeed, pristine graphene has no dangling bonds on its surface, inhibiting both the adsorption of the gaseous molecules of interest and the functionalization of species. Boron-doped graphene has also been studied for applications in other technological fields [8]. In fact, boron-doped graphene has been proposed as an active electrocatalyst for oxygen reduction reaction in fuel cells [9, 10], as a back electrode in CdTe solar cell [11], and as support for platinum catalyst [12]. For these last two applications, the boron-doped graphene samples were obtained from different types of thermal processing of graphene oxide.

Several approaches have been developed for the growth of graphene and the low-pressure chemical vapor deposition (LPCVD) technique which allows the acquisition of large-area high-quality graphene film [13]. The incorporation of boron atoms in graphene was obtained by different methods: exfoliation of boron-doped graphite [14], arc discharge of graphite electrodes in the presence of diborane [15], thermal decomposition of boron carbide powder [16], thermal annealing of graphene oxide in presence of boron oxide [9], hot filament CVD [17], and chemical vapor deposition (CVD) using solid or gas precursors [7, 18–23]. The CVD technique could produce a single layer of boron-doped graphene with an extremely toxic and inflammable gas, that is, diborane, as the precursor [21, 22]. On the other hand, pristine graphene, prepared by CVD using methane, can be doped by its exposure to diborane at a high temperature in a two-stage process [20]. Recently, Ruitao and collaborators proposed an alternative approach to the use of diborane [7]. As precursor for the CVD growth, they used a mixture of triethylborane and hexane. The results obtained diverge considerably from other results. In fact, while the STM results obtained by Wang and collaborators [19] indicated that boron atoms are primarily incorporated in graphene lattice in the graphitic form in a random distribution, the results obtained by Ruitao and collaborators [7] also using STM indicated the formation of boron-carbon trimmers embedded within the hexagonal lattice. In both cases, a p-type conducting behavior was verified. In the case of pristine graphene samples prepared by CVD and subsequently submitted to thermal annealing in a diborane atmosphere, boron-doped single-layer graphene was obtained with the presence of boron carbide nanoparticles at the grains boundaries [17]. Results for boron doping of single-layer graphene are still scarce and suggest that they are dependent on the parameters chosen for the CVD process.

In this work, boron-doped graphene was synthesized by low-pressure CVD (LPCVD) on copper foil substrates using a single liquid precursor, triisopropyl borate. We investigated the effects of the processing temperature and the vapor pressure in order to verify the homogeneity of the samples and optimize the growth parameters. The samples were characterized by Raman spectroscopy, X-ray photoelectron spectroscopy (XPS), optical microscopy, and field emission scanning electron microscopy (FEG-SEM). Our results show that, for the optimum conditions for single-layer graphene growth, that is, 1000°C and 75 mTorr for 5 minutes, we could obtain samples presenting the coexistence of pristine graphene with regions of boron-doped graphene, which is a different figure compared to previous boron-doped graphene prepared by CVD.

2. Materials and Methods

Boron-doped graphene was synthesized by the LPCVD method using copper foils as the substrate (25 μm thick from Alfa Aesar, 99.99% purity) and triisopropyl borate (from Sigma Aldrich, 98% purity) vapor as precursor. The processing temperature ranged from 900°C to 1000°C. The pressure was varied from 25 mTorr to 400 mTorr with a fixed exposure time of 5 minutes. The doped graphene was transferred to SiO_2 (300 nm thick)/Si and quartz substrates for subsequent characterizations using a wet transfer method with poly(methyl methacrylate) (PMMA) as the support film. Details of the sample preparation and transfer can be found elsewhere [24]. The liquid precursor volatizes when exposed to low pressures. The vapor was carried throughout the furnace using 2 sccm of H_2 gas. The boron-doped graphene was then synthesized by the self-assembly of the atoms dissociated from the vapor on the catalyst surface.

The samples were characterized using a multitechnique approach including micro-Raman spectroscopy (μRS), optical microscopy, scanning electron microscopy (SEM), and X-ray photoelectron spectroscopy (XPS). A micro-Raman spectrometer (NT-MDT, NTEGRA spectra) equipped with a CCD detector, cooled by a Peltier cell, and a solid-state laser, which provided an excitation wavelength of 473 nm (2.62 eV), was employed. Raman mapping was carried out by a piezoelectrically controlled XY table, which allowed for steps of 0.5 μm, coupled to a single grating (600 lines/mm) Raman spectrometer (HORIBA, LabRAM HR). This set-up was equipped with a He-Ne laser with an excitation wavelength of 633 nm (1.96 eV). In both systems, the laser spots on the sample surface were of the order of 0.5 μm, while to minimize the heating effects due to the laser irradiation we kept the incident beam power below 1 mW. Repeated Raman measurements were performed on different regions of the sample surface and the spectra from morphologically similar regions showed overall good reproducibility. Finally, the wavenumbers of the vibrational modes of O_2 (1555 cm^{-1}) and N_2 (2331 cm^{-1}) molecules in the air were exploited to calibrate the band position of the graphene spectra.

A field emission scanning electron microscope (FEG-SEM, JSM-6701 F, from JEOL) operating at 1 kV was employed for morphology analysis. X-ray photoelectron spectrometry (XPS) was carried-out using Mg K_α X-ray source ($h\nu$ = 1253.6 eV) and an Alpha 110 commercial hemispherical electron energy analyzer. The measurements were performed at a grazing angle of 80 degrees. The high-resolution XPS spectra were collected at a pass energy of 20 eV, and the data was processed using the CasaXPS software. It took the energy of the peak of C_{1s} at 284.5 eV as a reference.

A Zeiss Axio optical microscope was used for sample imaging, and the optical transmittance was measured in the range of 40 to 800 nm by using a UV-vis spectrophotometer (Lambda 950, Perkin Elmer, USA).

3. Results and Discussion

Typical Raman spectra recorded from samples grown using 25 mTorr of vapor pressure at three different temperatures in the 900°C–1000°C range and transferred to an oxidized silicon wafer via a PMMA route are shown in Figure 1. The spectra indicate that single-layer graphene was obtained at the highest temperature, 1000°C. The 2D band profiles of the samples deposited at the lower temperatures suggest that multilayer graphene was produced, while the presence of

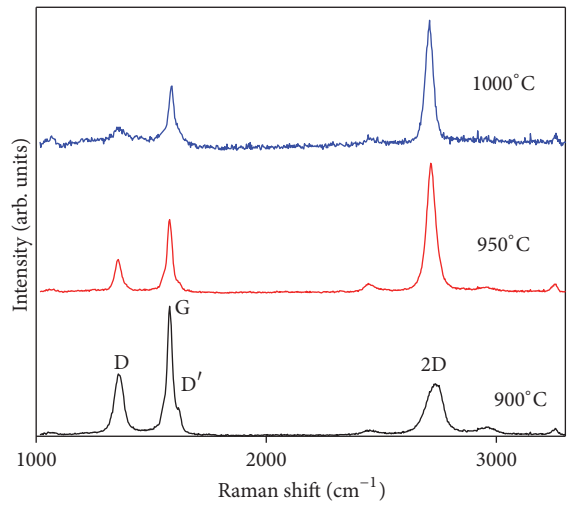

FIGURE 1: Raman spectra obtained from samples prepared under pressure of 25 mTorr at three different temperatures and transferred to SiO_2/Si via PMMA route.

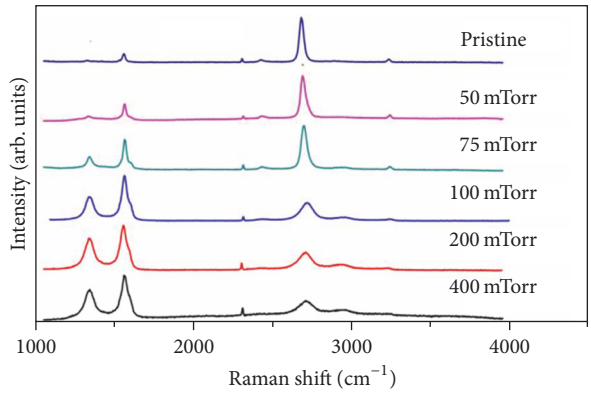

FIGURE 2: Raman spectra obtained from samples prepared at different pressures for 5 minutes at 1000°C and transferred to SiO_2/Si via PMMA route.

defects was revealed by the occurrence of the D peak. It became progressively more important for samples prepared at lower processing temperatures.

Figure 2 shows the spectra obtained from samples transferred to SiO_2/Si and prepared at different pressures. They were grown keeping the temperature and exposition time constant, 1000°C and 5 minutes, respectively. The Raman spectrum obtained from the samples prepared at 50 mTorr is quite similar to the spectrum of the pristine graphene layer obtained using methane as the precursor. In both spectra, the intensity ratio between the bands 2D and G (I_{2D}/I_G) is around 4, while the bandwidth of the 2D band is 35 cm^{-1}. These values are typical of good quality pristine samples. A very weak D-band was observed in these spectra. It can be reasonably attributed to defects introduced during the transfer procedure. The spectrum obtained from the samples grown at 75 mTorr shows a shoulder that corresponds to the D′ peak associated with the presence of defects. The other spectra of Figure 2 show an increase of the intensity of the D peak with the rise in the vapor pressure. The increase in the D-band suggests more defective samples and it is followed by a concomitant decrease in the I_{2D}/I_G intensity ratio. The spectra obtained from samples prepared at pressures higher than 75 mTorr are typical of nanocrystalline graphite, as revealed by the occurrence of a broad multiphonon band centered around 3000 cm^{-1} [25].

In Figure 3(a), we present the optical microscopy image obtained from a sample prepared at 75 mTorr and 1000°C for 5 minutes and transferred to a SiO_2/Si substrate, where the uniformity of the sample can be evaluated in the image. In Figure 3(b), we show the UV-vis transmittance of a sample prepared with the same parameters and transferred to a quartz substrate. Transmittance of the boron-doped sample is quite similar to that of pristine sample, also shown in the figure, and the transmitted value at 650 nm is 96.5 ± 0.2%. Based on previous reports, the experimental value for the transmittance of exfoliated graphene is 2.3 ± 0.1% [26]. The difference can be attributed to defects in both pristine and doped graphene generated during sample transfers to a quartz substrate. The presence of PMMA residues and the bilayer graphene covering small areas of the sample surface can also contribute to explaining this result.

Figure 4 shows the images of boron-doped graphene on copper grown at different triisopropyl borate vapor pressure. The samples were prepared at 1000°C for 5 minutes. Figure 4(a) corresponds to pristine graphene on copper used as the reference image for comparison purpose. For growth using 200 mTorr vapor pressure (image shown in Figure 3(d)), we obtained nanocrystalline graphite, confirmed by Raman spectra as shown Figure 2. For the 50 and 75 mTorr pressures, we see the formation of dark and bright domains. It is clear that the doped samples are not homogeneous at the 3 μm scale, while the pristine sample is homogenous at a much larger scale.

Raman mapping was exploited to probe the structural homogeneity of the samples. Figure 5(a) shows an optical image taken from a generic 60 μm × 50 μm region of the sample grown at 75 mTorr for 5 minutes at 1000°C. It shows some dark colored spots corresponding to PMMA residues, while the dashed rectangle (5 μm × 20 μm) is the region of the sample free of PMMA which was mapped.

The Raman map of the relative I_{2D}/I_G intensity ratio is highlighted in false colors and can be seen at the left side of the Raman spectra as an inset in Figure 5(b). The Raman spectra that are plotted in Figure 5(b) are those that have the extreme values for the I_{2D}/I_G (i.e., maximum) and I_{2D}/I_D (i.e., minimum) intensity ratios at points 1 and 2, respectively. The intersection of the red and blue lines indicates the exact point where each spectrum was recorded. In Figure 5(c), we plot only the regions of the spectra which correspond to the G- and D′-bands. The upshift in the G-band of the spectra obtained from point 2 is clear when compared to point 1. This is evidence of the p-doping of graphene, which is in agreement with the hole doping by applying a gate voltage [27]. The Raman map confirms the SEM images, since it shows that the sample consists of areas whose homogeneity is confined within a few microns square.

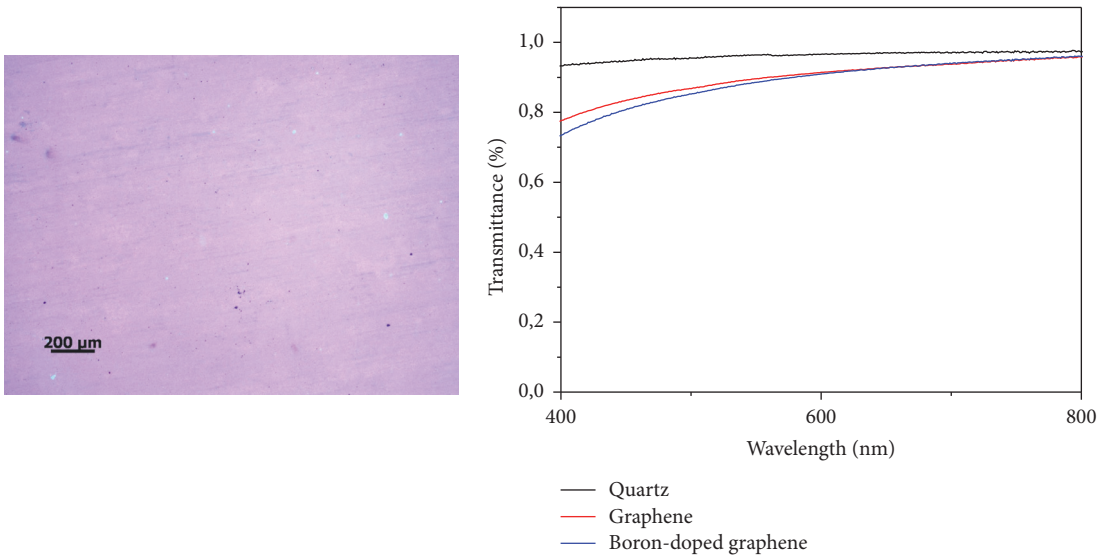

(a) (b)

FIGURE 3: (a) Optical microscopy image of doped graphene prepared at 75 mTorr, 1000°C, and 5 minutes and transferred to a SiO_2/Si substrate. (b) UV-vis transmittance of quartz substrate, pristine graphene, and doped graphene of a sample prepared with the same parameters and transferred to a quartz substrate.

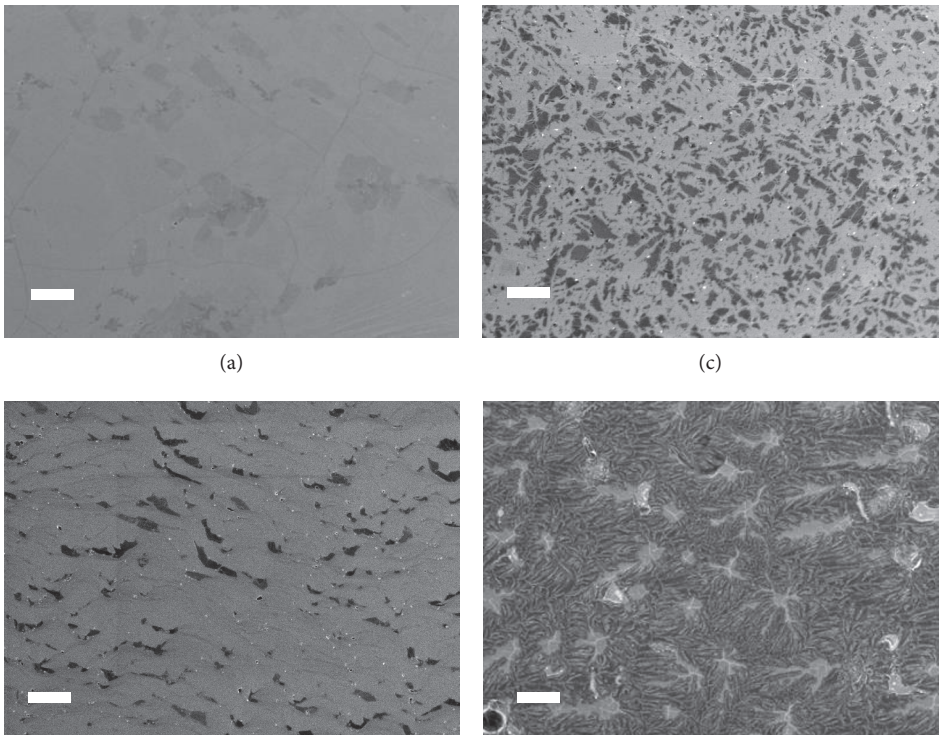

(a) (c)

(b) (d)

FIGURE 4: SEM images of (a) pristine graphene; (b) boron-doped graphene obtained at pressure of 50 mTorr, (c) 75 mTorr, and (d) 200 mTorr during 5 minutes at 1000°C. The scale bars of the images correspond to 3 μm.

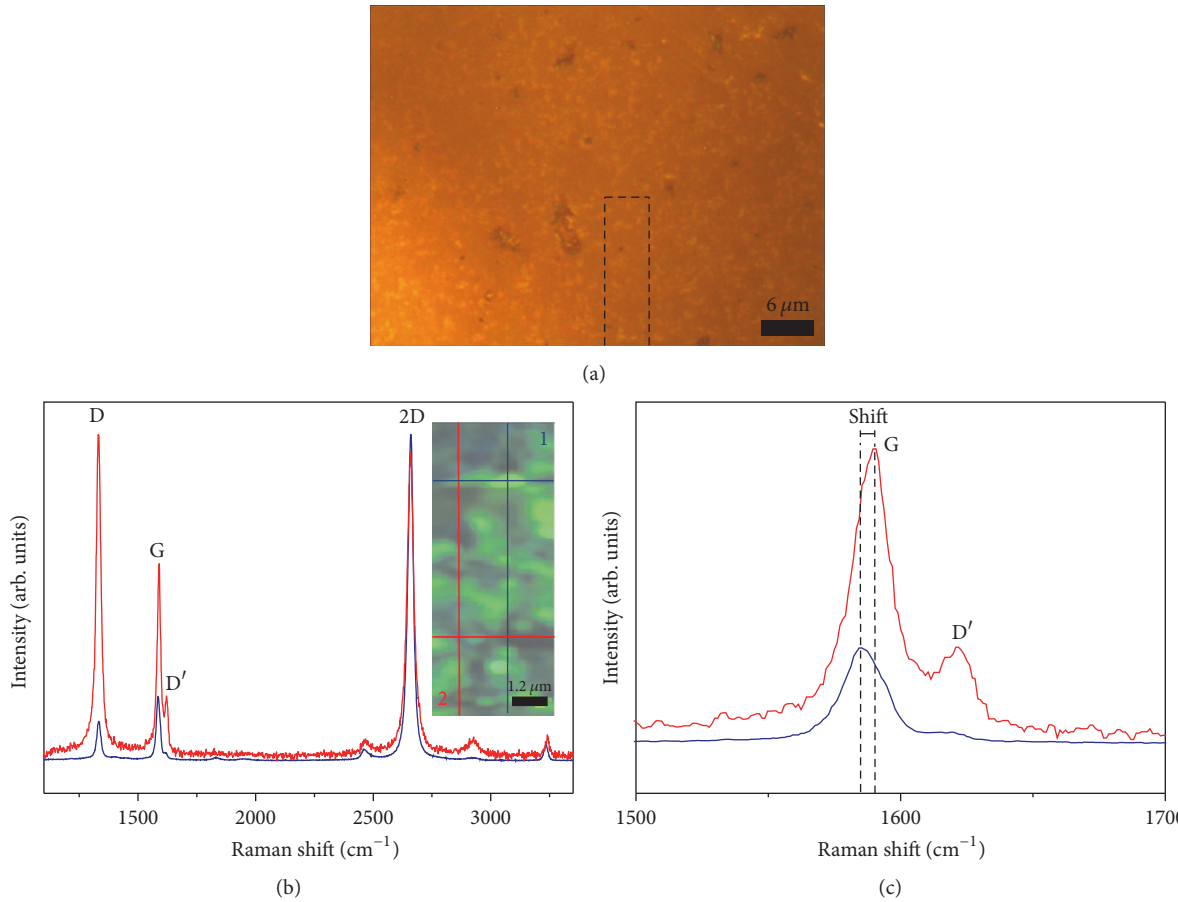

FIGURE 5: (a) Optical micrograph showing the portion (inside the dashed line) from which Raman mapping was carried out. (b) Raman spectrum with the highest value of the I_{2D}/I_G intensity ratio (blue) and with the lowest value of the same ratio (red). Note the presence of the D′-band centered at around 1620 cm^{-1}. (c) Raman spectrum of G-band showing the shift of the G-band of point 2 compared to point 1. The sample was prepared at 1000°C at 75 mTorr during 5 minutes.

In contrast, when one considers larger areas, the sample turns out to be not homogeneous. It is clear that the darker green zones correspond to the minimum value of I_{2D}/I_G, while the brighter green zones correspond to the maximum value of this ratio. In fact, the I_{2D}/I_G intensity ratio varied from 1.5 to 6.0 for the spectra obtained in the measured region, which is indicated in Figure 5(a). The blue and red spectra quoted in Figure 5(b) also correspond to the extreme values of the ratio between the D-band and G-band (I_D/I_G) but with the opposite behavior. In fact, I_D/I_G is the minimum for the spectrum obtained at point 1 (blue) and the maximum for the spectrum obtained at point 2 (red).

Another important parameter is the bandwidth of the 2D band. In both spectra, the bandwidths are around 30 cm^{-1} which is characteristic of single-layer graphene. Besides the difference in the I_{2D}/I_G ratio, other important features are the presence of the D′-band, as a peaked shoulder of the G-band, in the red spectrum plotted in Figure 5(b), as well as the ratio between the D- and G-bands. I_D/I_G is 0.6 for the blue spectrum and 1.8 for the red spectrum plotted in Figure 5(b). It was shown by theoretical calculations that both carbon and boron atoms can diffuse very rapidly on the copper surface and that boron atoms are incorporated at the growth edge forming pentagons [28]. Then, the concentration of topological defects (as pentagons) in boron-doped graphene must be very high [28], explaining the higher value of the I_D/I_G ratio and the presence of the D′-band in the Raman spectra.

The combination of these results indicates that we have a type of composite material, where the p-doped graphene layer (point 2) coexists with pure single-layer graphene regions (point 1) in Figure 5. In fact, the red spectrum presented in Figure 5(b) is similar to those previously reported in the literature for boron-doped graphene, grown from different precursors [7, 17]. The positions of the G-bands are slightly shifted toward a higher frequency, corroborating this picture.

The samples were also characterized by XPS. The carbon peak dominates the XPS survey spectrum obtained from graphene samples, with a small peak due to the presence of boron around 190 eV. Other peaks were also observed in the survey spectrum: the oxygen peak at 531 eV and the carbon and oxygen Auger peaks at 990 eV and 750 eV, respectively.

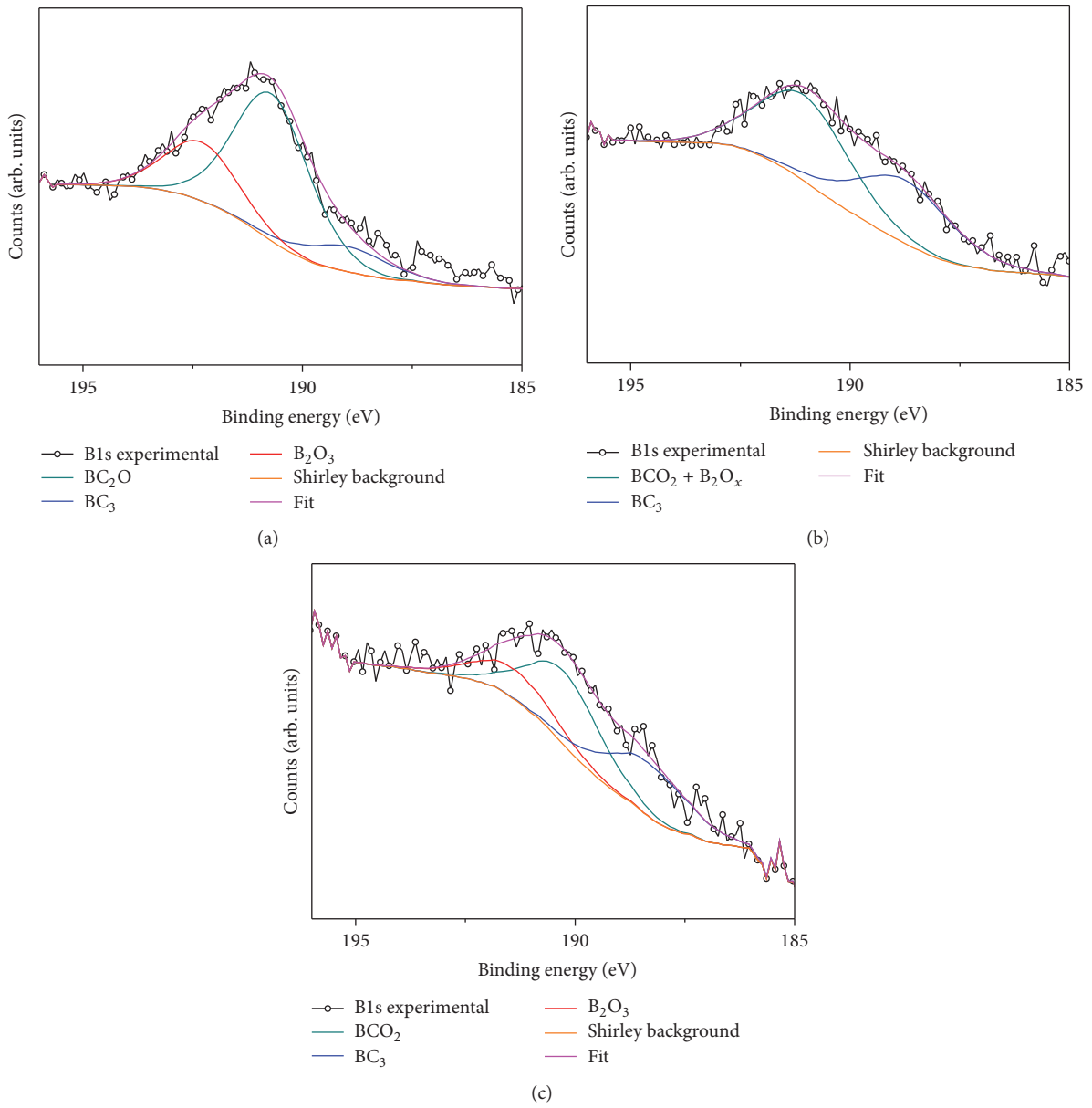

FIGURE 6: XPS B1s core-level spectrum of the samples grown using Cu substrate exposed during 5 minutes at 1000°C to (a) 200 mTorr, (b) 75 mTorr, and (c) 50 mTorr of triisopropyl borate vapor.

Typical XPS B1s core-level spectra are presented in Figure 6 for samples grown at 200, 75, and 50 mTorr vapor pressure for 5 minutes at 1000°C. The spectrum was decomposed in several contributions keeping the FWHM between 1.5 and 1.6 eV and assuming a Shirley background. One difficulty that arises is the question of determining the correct value for the binding energy in the substitutional doping of graphene with boron detected via photoemission spectroscopy induced by X-rays. Few theoretical studies have been reported in the literature. Based on DFT calculations, a value between 188.5 and 190 eV for the binding energy is attributed in the XPS B_{1s} core-level spectra revealing the boron incorporation into substitutional sites [29]. High-energy resolution XPS measurements on boron-doped graphene have associated the peak with a binding energy of 189.6 eV to substitutional doping of graphene by boron atoms [20]. Wu et al. [18] deconvoluted the B_{1s} spectrum of boron-doped graphene obtained by CVD from a solid precursor and assigned the peak with a binding energy of 189.7 eV to BC_3, the chemical environment of boron atoms in the case of substitutional boron doping. Thus, the peak having a binding energy of 189.4 eV can be attributed to sp^2 carbon-boron bonds in substitutional boron sites in graphene, in good agreement with previous XPS measurements [20]. The peak at 187.5 eV is associated with B_4C [30], while the two peaks corresponding to higher binding energies are assigned to BCO_2 at 191.5 eV

Table 1: XPS results of the samples prepared by CVD using Cu substrate exposed during 5 minutes to different vapor pressures of triisopropyl borate at 1000°C.

	Boron (at.%)	BC_3 (at.%)	BCO_2 (at.%)	BC_2O (at.%)	B_2O_3 (at.%)	B_4C (at.%)
50 mTorr	1.4 ± 0.3	0.6	0.3	—	0.5	—
75 mTorr	1.0 ± 0.3	0.4	0.5	—	—	—
200 mTorr	2.5 ± 0.5	0.4	—	1.5	0.6	—

[19] and B_2O_y at 193 eV [30], respectively, which can be formed when boron atoms adopt a low-coordination substitutional site close to the graphene edges [19, 20]. The peak at 190.7 eV is assigned to BC_2O compound in the sample grown at 200 mTorr [29].

In Table 1, the amounts of boron present in the samples grown using Cu substrate exposed at 25, 75, and 200 mTorr pressure of triisopropyl borate vapor at 1000°C for 5 minutes are reported. The total amount of boron is the range between 1 at.% and 2.5 at.% and the substitutional boron is around 0.4 at.%. In this case, we suggest that the substitutional boron is responsible for the doping.

4. Conclusions

In this work, single-layer graphene was synthesized using a low-pressure CVD system on copper foil substrates using triisopropyl borate vapor. Morphological results showed the formation of a kind of composite material, while Raman mapping confirms that the samples are not homogenous. The Raman results suggest that doped areas coexist with pure graphene areas. We also performed XPS measurements. The XPS spectra show the presence of not only substitutional boron but also boron bonded to oxygen and carbon (BC_xO_Y). The observed shift to higher frequencies of the G and 2D bands suggests the p-doping of single-layer graphene. In contrast with what was observed by Cattelan et al. [20], we attributed the composite character of the samples to a blend between doped graphene and undoped graphene, while they proposed the presence of boron carbide nanoparticles at the border grains of doped graphene. The other previous works did not analyze the homogeneity of the samples upon large areas. The lack of homogeneity appeared, from our results, to be the most important obstacle in the search for single-layer graphene doped with boron produced by different techniques, including CVD.

Additional Points

Highlights. We grow single-layer graphene using the liquid precursor triisopropyl borate. The XPS spectra show the presence of substitutional boron. SEM images suggested the formation of a composite material. Raman maps reveal the coexistence of pristine graphene with regions of doped graphene.

Conflicts of Interest

The authors declare that there are no conflicts of interest regarding the publication of this paper.

Acknowledgments

This work was partially supported by Brazilian agencies: CNPq, CAPES, FAPERJ, and the National Institute of Surface Engineering (INES). The authors are indebted to Arun Kumar for Raman mapping. Finally, one of the authors (G. Mariotto) acknowledges the financial support of the Brazilian program Science without Borders.

References

[1] F. Bonaccorso, V. Fal'ko, K. S. Novoselov et al., "Science and technology roadmap for graphene, related two- dimensional crystals, and hybrid systems," *Nanoscale*, vol. 7, pp. 4598–4810, 2015.

[2] T. B. Martins, R. H. Miwa, A. J. R. da Silva, and A. Fazzio, "Electronic and transport properties of boron-doped graphene nanoribbons," *Physical Review Letters*, vol. 98, no. 19, Article ID 196803, 2007.

[3] D. Usachov, O. Vilkov, A. Grüneis et al., "Nitrogen-doped graphene: efficient growth, structure, and electronic properties," *Nano Letters*, vol. 11, no. 12, pp. 5401–5407, 2011.

[4] M. S. Islam, K. Ushida, S. Tanaka, T. Makino, and A. Hashimoto, "Effect of boron and nitrogen doping with native point defects on the vibrational properties of graphene," *Computational Materials Science*, vol. 94, no. C, pp. 35–43, 2014.

[5] A. Salehi-Khojin, D. Estrada, K. Y. Lin et al., "Polycrystalline graphene ribbons as chemiresistors," *Advanced Materials*, vol. 24, no. 1, pp. 53–57, 2012.

[6] A. Cagliani, D. M. A. Mackenzie, L. K. Tschammer, F. Pizzocchero, K. Almdal, and P. Bøggild, "Large-area nanopatterned graphene for ultrasensitive gas sensing," *Nano Research*, vol. 7, no. 5, pp. 743–754, 2014.

[7] Lv. Ruitao, G. Chen, Q. Li et al., "Ultrasensitive gas detection of large-area boron-doped graphene," *PNAS*, vol. 112, p. 14527, 2015.

[8] S. Agnoli and M. Favaro, "Doping graphene with boron: a review of synthesis methods, physicochemical characterization, and emerging applications," *Journal of Materials Chemistry A*, vol. 4, no. 14, pp. 5002–5025, 2016.

[9] Z.-H. Sheng, H.-L. Gao, W.-J. Bao, F.-B. Wang, and X.-H. Xia, "Synthesis of boron doped graphene for oxygen reduction reaction in fuel cells," *Journal of Materials Chemistry*, vol. 22, no. 2, pp. 390–395, 2012.

[10] D.-Y. Young, W. Jeon, N. D. K. Tu et al., "High-concentration boron doping of graphene nanoplatelets by simple thermal annealing and their supercapacitive properties," *Scientific Reports*, vol. 5, article 9817, 2015.

[11] T. Lin, F. Huang, J. Liang, and Y. Wang, "A facile preparation route for boron-doped graphene, and its CdTe solar cell application," *Energy & Environmental Science*, vol. 4, no. 3, pp. 862–865, 2011.

[12] Y. Sun, C. Du, M. An et al., "Boron-doped graphene as promising support for platinum catalyst with superior activity towards the methanol electrooxidation reaction," *Journal of Power Sources*, vol. 300, pp. 245–253, 2015.

[13] X. Li, W. Cai, J. An et al., "Large-area synthesis of high-quality and uniform graphene films on copper foils," *Science*, vol. 324, no. 5932, pp. 1312–1314, 2009.

[14] Y. A. Kim, K. Fujisawa, H. Muramatsu et al., "Raman spectroscopy of boron-doped single-layer graphene," *ACS Nano*, vol. 6, no. 7, pp. 6293–6300, 2012.

[15] L. S. Panchakarla, K. S. Subrahmanyam, S. K. Saha et al., "Synthesis, structure, and properties of boron- and nitrogen-doped graphene," *Advanced Materials*, vol. 21, no. 46, pp. 4726–4730, 2009.

[16] W. Norimatsu, K. Hirata, Y. Yamamoto, S. Arai, and M. Kusunoki, "Epitaxial growth of boron-doped graphene by thermal decomposition of B4C," *Journal of Physics Condensed Matter*, vol. 24, no. 31, Article ID 314207, 2012.

[17] A. Jafari, M. Ghoranneviss, and A. Salar Elahi, "Growth and characterization of boron doped graphene by Hot Filament Chemical Vapor Deposition Technique (HFCVD)," *Journal of Crystal Growth*, vol. 438, pp. 70–75, 2016.

[18] T. Wu, H. Shen, L. Sun, B. Cheng, B. Liu, and J. Shen, "Nitrogen and boron doped monolayer graphene by chemical vapor deposition using polystyrene, urea and boric acid," *New Journal of Chemistry*, vol. 36, no. 6, pp. 1385–1391, 2012.

[19] H. Wang, Y. Zhou, D. Wu et al., "Synthesis of boron-doped graphene monolayers using the sole solid feedstock by chemical vapor deposition," *Small*, vol. 9, no. 8, pp. 1316–1320, 2013.

[20] M. Cattelan, S. Agnoli, M. Favaro et al., "Microscopic view on a chemical vapor deposition route to boron-doped graphene nanostructures," *Chemistry of Materials*, vol. 25, no. 9, pp. 1490–1495, 2013.

[21] J. Gebhardt, R. J. Koch, W. Zhao et al., "Growth and electronic structure of boron-doped graphene," *Physical Review B—Condensed Matter and Materials Physics*, vol. 87, no. 15, Article ID 155437, 2013.

[22] L. Zhao, M. Levendorf, S. Goncher et al., "Local atomic and electronic structure of boron chemical doping in monolayer graphene," *Nano Letters*, vol. 13, no. 10, pp. 4659–4665, 2013.

[23] S. Kamoi, J. G. Kim, N. Hasuike, K. Kisoda, and H. Harima, "Spectroscopic characterization of nitrogen- and boron-doped graphene layers," *Japanese Journal of Applied Physics*, vol. 54, no. 11, Article ID 115101, 2015.

[24] G. C. Mastrapa, M. E. H. M. da Costa, D. G. Larrude, and F. L. Freire, "Synthesis and characterization of graphene layers prepared by low-pressure chemical vapor deposition using triphenylphosphine as precursor," *Materials Chemistry and Physics*, vol. 166, pp. 37–41, 2015.

[25] R. J. Nemanich and S. A. Solin, "First- and second-order Raman scattering from finite-size crystals of graphite," *Physical Review B*, vol. 20, no. 2, pp. 392–401, 1979.

[26] R. R. Nair, P. Blake, A. N. Grigorenko et al., "Fine structure constant defines visual transparency of graphene," *Science*, vol. 320, no. 5881, p. 1308, 2008.

[27] A. Das, S. Pisana, B. Chakraborty et al., "Monitoring dopants by Raman scattering in an electrochemically top-gated graphene transistor," *Nature Nanotechnology*, vol. 3, no. 4, pp. 210–215, 2008.

[28] L. Wang, X. Zhang, F. Yan, H. L. W. Chan, and F. Ding, "Mechanism of boron and nitrogen in situ doping during graphene chemical vapor deposition growth," *Carbon*, vol. 98, pp. 633–637, 2016.

[29] F. H. Monteiro, D. G. Larrude, M. E. H. da Costa, L. A. Terrazos, R. B. Capaz, and F. L. Jr. Freire, "Production and characterization of boron-doped single wall carbon nanotubes," *The Journal of Physical Chemistry C*, vol. 116, no. 5, pp. 3281–3285, 2012.

[30] L. G. Jacobsohn, R. K. Schulze, M. E. H. Costa, and M. Nastasi, "X-ray photoelectron spectroscopy investigation of boron carbide films deposited by sputtering," *Surface Science*, vol. 572, no. 2-3, pp. 418–424, 2004.